THE JOURNAL OF PHYSICAL CHEMISTRY A

Article

Theoretical Study of the Complexes of Horminone with Mg and Ca Ions and Their Relation with the Bacteriostatic Activity

Ins Nicols, and Miguel Castro

J. Phys. Chem. A, **2006**, 110 (13), 4564-4573 • DOI: 10.1021/jp0565812

Theoretical Study of the Complexes of Horminone with Mg^{2+} and Ca^{2+} Ions and Their Relation with the Bacteriostatic Activity

Inés Nicolás[†,‡] and Miguel Castro*[,‡]

Coordinación de Posgrado, Facultad de Estudios Superiores Cuautitlán, Campo 1, Universidad Nacional Autónoma de México, Cuautitlán Izcalli, C.P. 54740, Estado de México, Mexico, and Departamento de Física y Química Teórica, DEPg Facultad de Química, Universidad Nacional Autónoma de México, Del. Coyoacán, México D.F., C.P. 04510 Mexico

Received: November 14, 2005; In Final Form: February 13, 2006

The coordination of the horminone molecule with hydrated magnesium and calcium divalent ions was studied by means of the density functional theory. All-electron calculations were performed with the B3LYP/6-31G method. The first layer of the water molecules surrounding the metallic cations was included. It was found that the octahedral $[horminone(O_a-O_d)-Mg-(H_2O)_4]^{2+}$ complex is more stable than $[Mg(H_2O)_6]^{2+}$. That is, horminone is able to displace two water units from the hexahydrated complex. This behavior does not occur for Ca^{2+}. Consistently, $[horminone(O_a-O_d)-Mg-(H_2O)_4]^{2+}$ has a greater metal−ligand binding energy than $[horminone(O_a-O_d)-Ca-(H_2O)_4]^{2+}$. The preference of horminone by Mg^{2+} is enlightened by these results. Moreover, its electronic structure, as shown by huge changes in the atomic populations, is strongly perturbed by Mg^{2+}. Indeed, horminone, bonded to $[Mg(H_2O)_4]^{2+}$, is able to cross the bacterial membrane cell. Once inside, $[horminone(O_a-O_d)-Mg-(H_2O)_4]^{2+}$ binds to rRNA phosphate groups yielding $[horminone(O_a-O_d)-Mg-(H_2O)(PO_4H_2)(PO_4H_3)_2]^+$. These results give insights into how horminone may inhibit the initial steps of protein synthesis. The stability of the studied systems is accounted for in terms of the calculated structural and electronic properties: Mg−O and Ca−O bond lengths, charge transfers, and binding energies.

1. Introduction

A fundamental problem in physical chemistry is to asses the activity of a given compound in terms of its structure or geometry and electronic properties. For instance, several approaches or protocols have been designed, such as QSAR or QSAR−CoMFA,[1−3] which require molecular parameters, obtained by quantum mechanical calculations, usually done with semiempirical and/or ab initio methods, for the treatment and characterization of the activity. These types of methods have proved to be useful when the number of molecular species, whose activity has been measured, is relatively large. Once the biological activity of a compound has been confirmed remains the determination, at the molecular level, of the involved mechanism during the action of a single molecule or drug. The study of this step requires the performance of ab initio quantum calculations, more accurate than the semiempirical ones, for a precise determination of the structural and electronic properties of the molecule or drug under study. This way, it is feasible, first, to locate the compound active site and, second, to study how the interaction with the receptor precedes, usually a small region of a macromolecule, such as rRNA. The purpose of this paper is to present a theoretical study, done ab initio, for the horminone molecule, which has the property of inhibiting the growth of several types of bacteria.[4] An attempt is made to characterize the key parameters, structural and electronic, involved during the bacteriostatic activity of such compound. The horminone molecule is a very important antibiotic. It was found for the first time in horminium pyrenaicum;[5] although prior to this it was known as semisynthetic substance.[6] Horminone has showed higher antibacterial activity against *Staphylococcus aureus* and *Vibrio cholerae*.[7] Its effect against *Bacillus subtilis* and *S. aureus* can also be considered as an intermediate susceptibility level against these type of bacteria.[8] Other studies have demonstrated that this molecule has been active against *Staphylococcus* epidermidis.[9] Moreover, it was also found to be cytotoxic against mammalian tumor cells[10] and also behaves as inhibitor against *Trypanosoma cruzi* growth, the Chagas disease agent.[11] Regarding its structure, horminone, an abietan diterpene quinone, is related to tetracycline, specifically to oxytetracycline, a well-known commercial antibiotic.[4,12,13] It is worthwhile to mention that the physical chemistry of these kinds of compounds has been scarcely studied, despite their clinical importance.[14] It has been observed that tetracycline is a metal-dependent antibacterial agent that inhibits bacterial protein synthesis by binding to the ribosome. In the extracellular form is likely to exist either as a Mg^{2+} or Ca^{2+} complex since both the binding affinities and the extracellular concentrations of Mg^{2+} and Ca^{2+} are similar (1 mM vs 4 mM).[15] With respect to the microbiological action of tetracyclines, Mg^{2+} and Ca^{2+} are probably the most relevant divalent cations to be considered for chelation. Mg^{2+} is the dominant divalent cation (2 mM) in the intracellular environment ($pH \leq 6.6$), where the concentration of Ca^{2+} is significantly lower (0.1 μM).[16] It is well-known that inside cells free metal ion concentrations are much lower than the total metal ion concentrations, meaning that intracellular macromolecules bind substantial amounts of metal ions.[17] The coordination number and coordination geometry depend on characteristics of both the metal ion and the ligands. The aqueous Mg^{2+} and Ca^{2+} ions considered here are frequently hexacoordinate complexes where the six-coordinated moieties are located at the apexes of an octahedron. Metal ions show differences in

* Corresponding author. E-mail: castro@quetzal.pquim.unam.mx.
† Facultad de Estudios Superiores Cuautitlán, Universidad Nacional Autónoma de México.
‡ DEPg Facultad de Química, Universidad Nacional Autónoma de México.

10.1021/jp0565812 CCC: $33.50
Published on Web 03/16/2006

the preferred patterns in coordination complexes. On the basis of these preferences, both metal ions and ligands can be classified as "hard" or "soft". In solutions, hard metal ions preferentially bind hard molecular species and soft metal ions preferentially bind soft molecules. For the purpose of RNA studies, those moieties that coordinate through sulfur or nitrogen atoms are considered soft and those coordinating through oxygen are considered hard.

In this regard, we recently studied the interaction, in the gas phase, of the horminone molecule with a single divalent magnesium cation, Mg^{2+}.[18] In fact, the interaction of horminone (Hm) with this metallic ion is very important, since it may be the responsible for the obtainment of an "active molecule", through the modification of its physical chemistry properties. For instance, it is believed that, through the Hm−Mg^{2+} complex, the horminone moiety is able to cross the bacterial wall cell; once inside the inhibition mechanism of the protein synthesis is switched-on. On the other hand, it has been recognized that the hexahydrated Mg^{2+} ion is involved in a structural role when it is associated with proteins.[19] So, it is very important to understand the bonding behavior of horminone with hydrated Mg^{2+} and Ca^{2+} cations, since both ions are present in the bacteria. As it was mentioned above, the purpose of this contribution is to report a density functional theory (DFT) study for the complexation of horminone with the hydrated magnesium and calcium divalent cations. The most favorable sites for coordination were determined, and the Hm−Mg^{2+} and Hm−Ca^{2+} complexes contain the direct effects of the first layer of the solvent water molecules.

Aside from the determination of the structural, electronic, and energetic properties of the hydrated Hm−Mg^{2+} complex, we have also addressed the study on a proposal for the structure of the hydrated horminone magnesium complex bounded at the macromolecules region (i.e. rRNA 30S) responsible for some steps (i.e. decoding process) during the proteins synthesis.[20] In fact, most ribosomal antibiotics work by binding to specific sites, i.e., the ribosome phosphate groups, and interfering with ribosome function during the protein synthesis. For example, there is evidence that this type of bacteriostatic action is shown by some tetracyclines.[20] Since horminone is structurally correlated to oxytetracycline, it is expected that the former molecule will exhibit a similar bacteriostatic behavior as the last compound, which has been widely studied. In this regard, the structural and electronic properties of Hm−Mg^{2+}−phosphate are needed to obtain an understanding of how this antibiotic interacts, with the ribosome, at molecular level.

It has been found, for oxygen donor monodentate ligands, that octahedral six coordination, $[Mg(H_2O)_6]^{2+}$, is dominant for the Mg^{2+} complexes,[19,21,22] while, for Ca^{2+}, the most common coordination numbers range from 6 to 9.[23,24] Moreover, some theoretical studies show that $[Mg(H_2O)_6]^{2+}$ is more stable than $[Ca(H_2O)_6]^{2+}$.[25] As it is well-known, Mg^{2+} and Ca^{2+} ions are very important in several biological processes. Then, we are interested in studying the interaction of these hydrated ions with horminone and on determining which cation is more favorable, by means of a total energy criteria, for the binding with this antibiotic. For this purpose, aside from $[Mg(H_2O)_6]^{2+}$ and $[Ca(H_2O)_6]^{2+}$, we have studied the [horminone−Mg−$(H_2O)_4$]$^{2+}$ and [horminone−Ca−$(H_2O)_4$]$^{2+}$ systems. In the case of the tetracycline antibiotic, it has been found that the divalent magnesium is crucial for the binding of this molecule to the ribosome. That is, this drug interacts with the phosphate oxygen atoms of the RNA residues,[20] promoting the inhibition of the protein synthesis. Therefore, we have also studied the [horminone−Mg−$(H_2O)(PO_4H_2)(PO_4H_3)_2$]$^{+}$ system. The stability of these complexes is addressed in terms of the calculated structural and electronic parameters, namely Mg−O and Ca−O bond lengths, charge transfers, and binding energies. The obtained results give insight into the role played by horminone during the inhibition of the protein synthesis.

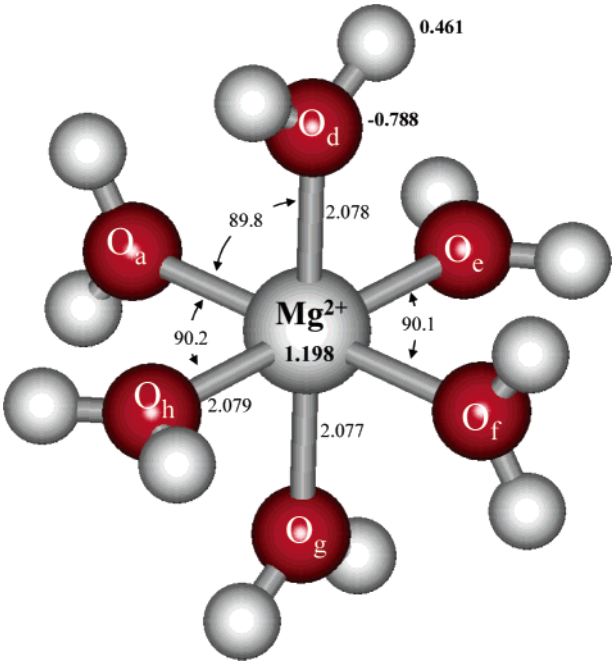

Figure 1. Selected geometrical parameters from the B3LYP/6-31G optimized structure. Bond lengths are in Å and bond angles are in deg (in italics), and Mulliken charges, electron units (in bold characters), are indicated.

2. Computational Procedure

In this research, the geometry and the electronic structure for the lowest energy states of $[Mg(H_2O)_6]^{2+}$, $[Ca(H_2O)_6]^{2+}$, horminone, [horminone−Mg]$^{2+}$, [horminone−Ca]$^{2+}$, [horminone−Mg−$(H_2O)_4$]$^{2+}$, and [horminone−Ca−$(H_2O)_4$]$^{2+}$ were studied by means of all-electron calculations using the hybrid B3LYP functional[26,27] in concert with the 6-31G basis set.[28] Particularly, the hexahydrated cations were also fully optimized with the bigger 6-311+G(2d), 6-311+G(d,p), and 6-311+G(2d,2p) basis sets,[29] while the biggest basis set under which the horminone moiety was treated was 6-311+G(d,p), aside from the use of the 6-31G, 6-31G*, and 6-31G**[30] basis sets. Calculations were performed with the aid of the Gaussian-98 program.[31] Basis set superposition errors (BSSE) were estimated by the counterpoise method.[32] The optimized structures were confirmed as local minima by estimating their normal vibrations within the harmonic approximation. Charge distributions, through Mulliken population analysis, were determined for the equilibrium geometries. The structures and the molecular orbitals (MOs) were visualized through the GV package, coupled to Gaussian-98. In particular, MO frontiers, the so-called highest occupied molecular orbital (HOMO) and lowest unoccupied molecular orbital (LUMO), as well as the charge distributions, are very useful parameters that allow, in a first approach, the characterization of these antibiotic reactivities. Finally, the Bader theory "atoms in molecules" (AIM) was used to characterize some intramolecular hydrogen-bonding interactions in the horminone molecule.[33] AIM calculations based on the Bader theory were performed using the AIM2000 program.[34]

TABLE 1: Calculated M−O Bond Lengths, in Å, and O−M−O Bond Angles, in deg, for the $[M(H_2O)_6]^{2+}$ (M = Mg, Ca) Optimized Complexes Using B3LYP and the Indicated Basis Set

	$[Mg(H_2O)_6]^{2+}$				$[Ca(H_2O)_6]^{2+}$			
	6-31G	6-311+G(2d)	6-311+G(d,p)	6-311+(2d,2p)	6-31G	6-311+G(2d)	6-311+G(d,p)	6-311+(2d,2p)
				Bond				
M−O	2.078	2.098	2.111	2.100	2.407	2.398	2.402	2.403
M−O	2.078	2.097	2.111	2.100	2.407	2.399	2.403	2.404
M−O	2.078	2.097	2.110	2.100	2.409	2.401	2.404	2.405
M−O	2.079	2.098	2.111	2.101	2.409	2.400	2.404	2.405
M−O	2.077	2.099	2.112	2.101	2.410	2.402	2.406	2.407
M−O	2.079	2.098	2.111	2.101	2.411	2.403	2.406	2.407
O−H	0.975	0.969	0.967	0.965	0.976	0.969	0.968	0.966
				Angle				
O−M−O	89.8	90.0	90.0	90.0	89.2	90.7	90.6	90.6
O−M−O	90.2	90.0	90.0	90.0	91.0	89.6	89.6	89.6
O−M−O	90.2	90.0	90.1	90.1	90.3	89.9	89.9	90.0
O−M−O	90.2	90.0	90.0	90.0	88.6	91.2	91.1	91.1
O−M−O	89.9	90.1	90.1	90.1	89.3	90.5	90.5	90.5
O−M−O	90.2	89.9	89.9	89.9	89.9	90.9	90.8	90.8
O−M−O	90.1	90.2	90.1	90.1	91.3	89.3	89.4	89.4
O−M−O	89.8	90.1	90.1	90.1	89.1	89.2	89.2	89.3
O−M−O	90.0	89.8	89.8	89.8	89.5	90.2	90.2	90.2
O−M−O	90.0	89.8	89.9	89.9	90.9	89.4	89.4	89.5
O−M−O	90.2	90.1	90.1	90.1	90.6	90.3	90.3	90.3
O−M−O	89.8	89.8	89.8	89.8	90.2	88.8	88.9	88.9

3. Results and Discussion

$[Mg(H_2O)_6]^{2+}$ and $[Ca(H_2O)_6]^{2+}$. First, the geometry and electronic structure for the lowest energy states of the $[Mg(H_2O)_6]^{2+}$ and $[Ca(H_2O)_6]^{2+}$ complexes were calculated. Then, the capability of the horminone molecule for interacting with and displacing two water units from these hydrated systems was addressed. As it was mentioned, an octahedral hexacoordination was found to be dominant for Mg^{2+} interacting with monodentate ligands.[19,21,22] Our computed B3LYP/6-31G geometry for $[Mg(H_2O)_6]^{2+}$ is shown in Figure 1. In fact, this structure has an octahedral shape, with O−Mg−O bond angles very close to 90°. The Mg−O bond lengths, of 2.077−2.079 Å, Table 1, match the Mg−O value, of 2.08 Å, obtained by Pavlov et al. with the B3LYP/LAND2DZ method.[25] From the experimental side, it has been found that all the crystallographically determined Mg^{2+} aqua ions are six-coordinated,[24] with an average 2.066(2) Å Mg−O bond length. Our calculated Mg−O distance as well as that of ref 25 is in agreement with the experiment. On the other hand, for bare H_2O, the calculated O−H bond lengths and the H−O−H bond angle are equal to 0.975 Å and 110.25°, respectively. Then, with respect to the free water molecules and at the B3LYP/6-31G level of theory, the Mg−OH_2 bond formation produces a negligible shortening, ≅0.001 Å, of the bond lengths and an increase, ≅2°, of the angles, of the coordinated H_2O molecules. That is, the effect of Mg^{2+} on the geometry of the bounded water moieties is very small. Similar effects were obtained using bigger 6-311+G(2d), 6-311+G(d,p), and 6-311+G(2d,2p) basis sets.

The relatively short Mg−O bond length indicates a substantial bonding interaction among the water molecules and the metallic cation. A 399.2 kcal/mol binding energy**,** Table 2, was estimated for $[Mg(H_2O)_6]^{2+}$ (to the sum of the total energies of Mg^{2+} and six H_2O molecules was subtracted the total energy of the hexahydrated Mg^{2+} complex). After the inclusion of zero point energy (ZPE) corrections, a value of 380.31 kcal/mol is obtained. The strength of this metal−ligand bond is accounted by the magnitude of the charge transfer, of ≅0.8 electrons, which is carried out from the water moieties toward the metallic cation. Using a bigger basis set, Pavlov et al. have found, including ZPE corrections, a total binding energy of 303.9 kcal/mol and a charge transfer of ≅0.7 electrons.[25] In our all-electron calculations, the use of the 6-311+G(2d) basis yields a binding energy of 327.8 kcal/mol. After the inclusion of ZPE corrections, a value of 313.1 kcal/mol is obtained. Similarly, the bigger 6-311+G(d,p) and 6-311+G(2d,2p) basis sets give, including ZPE, binding energies of 309.02 and 303.23 kcal/mol, respectively. Note that 6-311+G(2d), 6-311+G(d,p), and 6-311+G(2d,2p) produce binding energies that differ by 10 kcal/mol. The last value, 303.23 kcal/mol, is remarkably close to the value reported by Pavlov et al.[25] In other words, the expensive calculation with the second, (2d,2p), set of polarization functions produces relatively small effects, with respect to the (2d) and (d,p) patterns, on the calculated energetic properties. These results point out that reasonably accurate geometries are obtained with the use of the relatively small 6-31G basis set, as quoted above with the results of the Mg−O bond lengths for $[Mg(H_2O)_6]^{2+}$. But an improvement in the binding energies needs a bigger 6-311+G(2d), 6311+G(d,p), or 6-311+G(2d,2p) basis set.

TABLE 2: Binding Energies (BE) and Total ZPE Corrected Binding Energies (BE-ZPE) for the $[M(H_2O)_6]^{2+}$ (M = Mg, Ca) Complexes, According to $[E(M^{2+}) + 6E(H_2O)] - E[M(H_2O)_6]^{2+}$, Using B3LYP and the Indicated Basis Set

basis set	BE-ZPE (kcal/mol)	BE (kcal/mol)
	$[Mg(H_2O)_6]^{2+}$	
6-31G	399.22	380.31
6-311+G(2d)	327.79	313.13
6-311+G(d,p)	324.06	309.02
6-311+(2d,2p)	317.62	303.24
	$[Ca(H_2O)_6]^{2+}$	
6-31G	301.49	288.10
6-311+G(2d)	252.47	240.79
6-311+G(d,p)	252.10	239.34
6-311+(2d,2p)	242.74	231.08

In the calculated B3LYP/6-31G lowest energy structure of $[Ca(H_2O)_6]^{2+}$, Figure 2, the Ca−O 2.41 Å bond length is significantly longer, 0.33 Å, than the Mg−O value, indicating a weaker metal−oxygen bonding interaction in the calcium complex. In fact, our calculated total binding energy, 301.5 or 288.10 kcal/mol including ZPE corrections, for $[Ca(H_2O)_6]^{2+}$, is smaller than the corresponding value for the Mg^{2+} complex. This result is consistent with the occurrence of a smaller charge transfer, of 0.55 electrons, from the H_2O moieties toward the

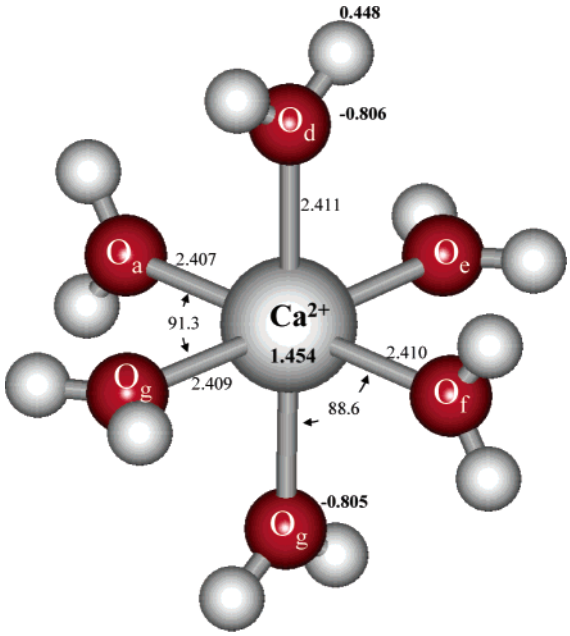

Figure 2. Selected geometrical parameters from the B3LYP/6-31G optimized structure. Bond lengths are in Å and bond angles are in deg (in italics), and Mulliken charges, electron units (in bold characters), are indicated.

Ca^{2+} cation. It is to be mentioned that our all-electron calculations with the bigger 6-311+G(2d), 6-311+G(d,p), and 6-311+G(2d,2p**)** basis sets produce total binding energies, including ZPE corrections, of 240.79, 239.34, and 231.10 kcal/mol, respectively; the last value is in close agreement with the result, 234.4 kcal/mol, reported by Pavlov et al.[25] These 6-311+G(2d) and 6-311+G(2d,2p) calculated binding energies are close to each other, but they are substantially smaller, by about 40−50 kcal/mol, than the 6-31G result. Moreover, all these $Ca^{2+}(H_2O)_6$ binding energies are smaller than their counterparts for the $Mg^{2+}(H_2O)_6$ case. So, the Mg^{2+} ion shows stronger bonding interactions with the monodentate water molecules than Ca^{2+}.

Our computed 6-31G Ca−O equilibrium bond length, 2.410 Å, is in reasonable agreement with the theoretical estimation, of 2.42 Å, obtained by Pavlov et al., at the B3LYP/LAND2DZ level of theory. They also report a charge transfer of 0.54 electrons from the water moieties toward the Ca^{2+} cation. Even more, these authors have observed that the calculated Ca−O bond distance using double-ζ type LANL2DZ basis sets is longer than the corresponding experimental value,[24] of 2.334-(9) Å. Since a reduction of 0.05 Å was obtained for the Ca−O bond length when d functions were added, a corrected value of 2.37 Å was reported in ref 25 for the Ca−O bond length in the $[Ca(H_2O)_6]^{2+}$ complex. In our calculations, the use of bigger 6-311+G(2d), 6-311+G(d,p), and 6-311+G(2d,2p) basis sets produce bond lengths of 2.401, 2.404, and 2.405 Å, respectively. So, the use of these bigger basis sets produce an improvement, with respect to the 6-31G value, of only 0.005−0.009 Å for the Ca−O bond length in the $[Ca(H_2O)_6]^{2+}$ complex. But it is to be remarked that the use of the huge 6-311+G(2d), 6-311+G-(d,p), and 6-311+G(2d,2p) basis sets is prohibitive for calculations of many-electron systems where the horminone molecule replaces two water molecules. As shown above, the relatively small 6-31G basis produces geometries of reasonable accuracy for the Mg^{2+} and Ca^{2+} water complexes.

In summary, the B3LYP/6-31G binding energy results indicate that $[Mg(H_2O)_6]^{2+}$ is more stable, by ≅92.2 kcal/mol, than $[Ca(H_2O)_6]^{2+}$. The three methods, B3LYP/6-311+G(2d), B3LYP/6-311+G(d,p), and B3LYP/6-311+G(2d,2p), indicate that the former is more stable, by 72.3, 69.7, and 72.1 kcal/mol, respectively**.** Using the B3LYP functional and the 6-311+G-(2d,2p) basis, Pavlov et al. have also found that the octahedral $[Mg(H_2O)_6]^{2+}$ complex is more stable, by 70 kcal/mol, than $[Ca(H_2O)_6]^{2+}$. That is, DFT calculations reveal that the water−magnesium(II) complexes are more stable than the calcium(II) ones. As quoted, in a bacterial cell, there are both divalent cations. Now, we will analyze if horminone, which is a bidentade ligand, is able to displace two water molecules from the Mg^{2+}- and Ca^{2+}-hexahydrated complexes. The relative stability of the Ca^{2+}− and Mg^{2+}−horminone compounds will also be addressed.

[Horminone−M]$^{2+}$, M = Mg^{2+} and Ca^{2+}, Systems. The calculated electronic structure for the lowest energy state of horminone, indicates that the oxygen O_a and O_d atoms are the most negative sites of the molecule, since they have Mulliken populations of −0.61 and −0.45 electrons, respectively. See Figure 3. Also the O_b and O_c atoms are negative, with populations of −0.45 and −0.60 electrons. On the other hand, the hydrogen atom H_c, with +0.40 electrons, is the most positive atom, and H_a is also positive, with +0.38 electrons. Then, H_c and H_a are highly acid atoms. Consistent with this picture, the ground-state geometry of horminone reveals the appearance of two relatively strong intramolecular hydrogen bonds, O_b-H_c and O_d-H_a, with 2.009 and 2.136 Å distances, respectively. This H-bond formation was verified by AIM calculations, which indicated bond critical points along O_b-H_c and O_d-H_a; see Figure 3. Note that the O_b-H_c bond involves the formation of the five $O_b-H_c-O_c-C_{12}-C_{11}$ member ring, while O_d-H_a is associated with the formation of the six $O_d-H_a-O_a-C_7-C_8-C_{14}$ member cycle. Ring critical points were also found on these cycles by the AIM formalism. Concerning the molecular orbital description, it was found that the HOMO is mainly located on the quinone ring C, with some important contributions on the O_a and O_d atoms. See Figure 4, where the frontier molecular orbitals of horminone are shown. It can be observed that the HOMO-1 level, lying only 0.22 eV below HOMO, is also located on the quinone region, displaying also significant contributions, greater than those of HOMO, on the O_a and O_d atoms. Moreover, HOMO-2, lying 0.38 eV below HOMO-1, also presents strong contributions on the O_a and O_d sites. That is, these three orbitals may contribute to the coordination, through the horminone O_a and O_d atoms, with the Mg^{2+} or Ca^{2+} cations. This orbital cooperative effect, coupled with high negative charges on the O_a and O_d atoms, quoted above, produces a high nucleophilic character on these sites, needed for to displace two water moieties from $[Mg(H_2O)_6]^{2+}$ or $[Ca-(H_2O)_6]^{2+}$. Even more, the LUMO orbital is also mainly located on the quinone ring, with some contributions on the oxygen atoms, O_a and O_d. That is, the frontier molecular orbitals (LUMO, HOMO, HOMO-1, and HOMO-2) suggest that the O_a-O_d region may be considered as the reactive site of the horminone bidentade ligand, when it behaves as a nucleophile against acid centers, such as Mg^{2+} and Ca^{2+}. Indeed, total energy results indicate that the $Mg-O_a-O_d$ coordination mode is energetically more favored, since the $Mg-O_b-O_c$ mode was located 32.4 kcal/mol higher in energy.[18] Further, both [horminone(O_a-O_d)−Mg]$^{2+}$ and [horminone(O_b-O_c)−Mg]$^{2+}$ systems were calculated taken into account solvent effects through a self-consistent reaction field model; in particular, Tomasi's polarized continuum model (PCM)[35] was used. This way, the total energy difference between these complexes indicates that they are separated by a substantially smaller separation, of 8.0

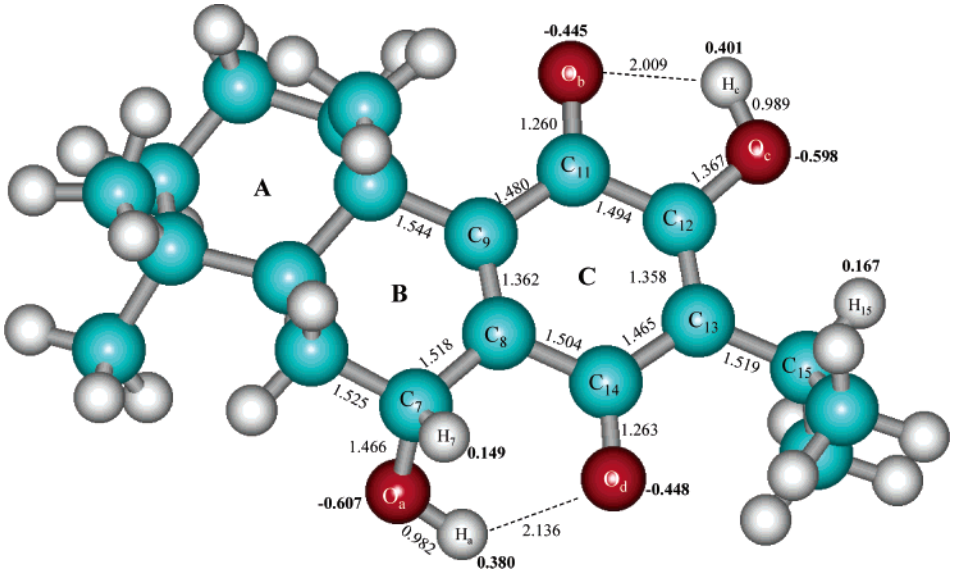

Figure 3. Selected geometrical parameters from the B3LYP/6-31G optimized structure. Bond lengths are in Å, and Mulliken charges, electron units (in bold characters), are indicated. The dashed lines indicate the intramolecular H-bond interaction, between H_a---O_d and H_c---O_b.

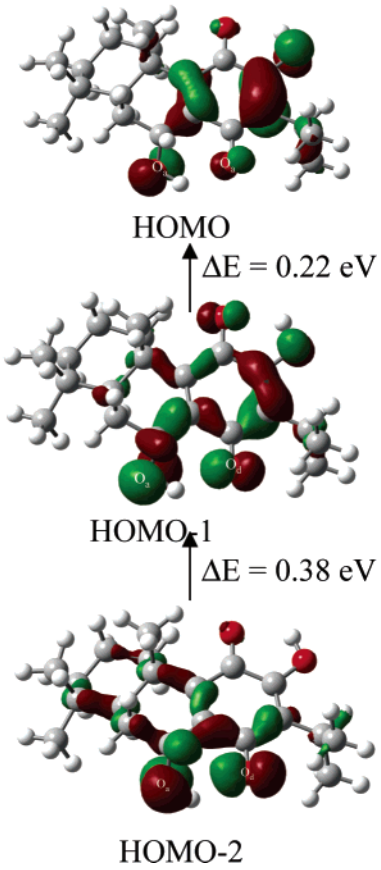

Figure 4. HOMO, HOMO-1, and HOMO-2 contour plots for the horminone molecule at the B3LYP/6-31G level.

kcal/mol, than that in the gas phase, with the Mg−O_a−O_d coordination mode remaining lower in energy than Mg−O_b−O_c. That is, both gas phase and PCM calculations indicate the same lowest energy state for the horminone−Mg^{2+} complex. In the next section we will include the solvent effects directly on these two coordination modes.

For [horminone−Ca]$^{2+}$, the lowest energy state also corresponds to the coordination of the Ca^{2+} cation with the O_a and O_d horminone atoms. The Ca−O_b−O_c mode was found 25.68 kcal/mol higher in energy; see Figure 5. In the preferred Ca−O_a−O_d state, the Ca−O_a (2.30 Å) and Ca−O_d (2.21 Å) bond lengths are noticeable longer than their counterparts of [horminone(O_a−O_d)−Mg]$^{2+}$, Mg−O_a (1.90 Å) and Mg−O_d (1.86 Å).

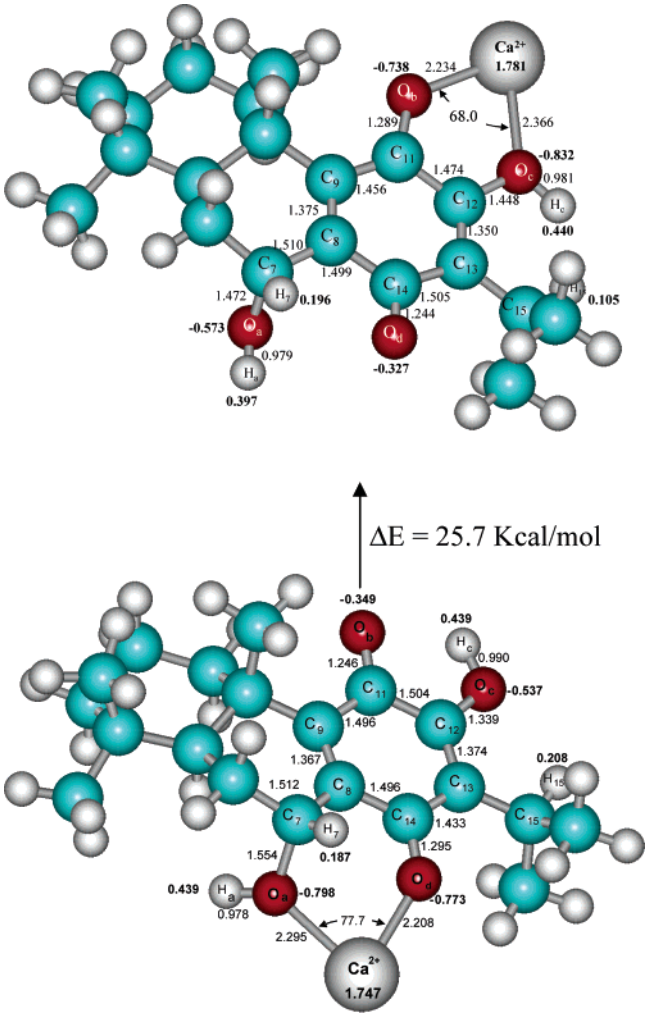

Figure 5. Optimized geometry for the [horminone(O_7−O_{14})−Ca]$^{2+}$ and [horminone(O_{11}−O_{12})−Ca]$^{2+}$ systems. Bond lengths, in Å, bond angles, in deg (in italics), and Mulliken populations, electron units (in bold characters), are indicated at the B3LYP/6-31G level.

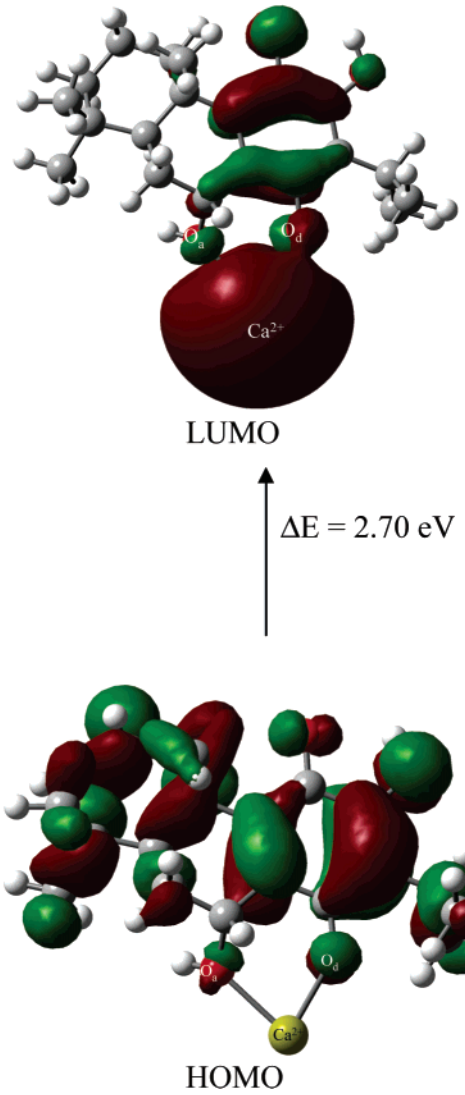

Figure 6. HOMO and LUMO contour plots for the [horminone(O_7−O_{14})−Ca]$^{2+}$ system using the B3LYP/6-31G level.

It can also be observed that the six-member ring Ca^{2+}−O_a−C_7−C_8−C_{14}−O_d, see Figure 5, is significantly more distorted, i.e., less planar, than the corresponding ring for Mg^{2+}−horminone. In fact, the Mg^{2+} ion promotes the formation of a quasi-planar Mg^{2+}−O_a−C_7−C_8−C_{14}−O_d ring.

The HOMO and LUMO contour plots for the [horminone-(O_a−O_d)−Ca]$^{2+}$ lowest energy state are shown in Figure 6. Note that the LUMO presents strong contributions on the quinone ring **C** and on the Ca^{2+} region. In the quinone region **C**, the HOMO displays a pattern similar to that of free horminone, except that now appears some significant contributions on the cyclohexyl group **A**. In contrast, in [horminone(O_a−O_d)−Mg]$^{2+}$ the HOMO is more strongly displaced from **C** toward the **A** ring, while the LUMO is highly located on the Mg^{2+} region, with some small contributions on the O_a−C_7−C_8−C_{14}−O_d atoms. That is, the LUMOs of [horminone(O_a−O_d)−Ca]$^{2+}$ and of [horminone(O_a−O_d)−Mg]$^{2+}$ present appropriate channels for their bonding interaction with nucleophilic molecules, such as water or phosphate moieties.

Overall, these results indicate a weaker bonding behavior in Ca^{2+}−horminone than in Mg^{2+}−horminone. This can be rationalized in terms of the transferences of charge that occur from horminone toward the metallic ions. In the Ca complex, the transference, 0.25 electrons, is half from that observed for the Mg^{2+} case. In fact, the metal−ligand binding energy for

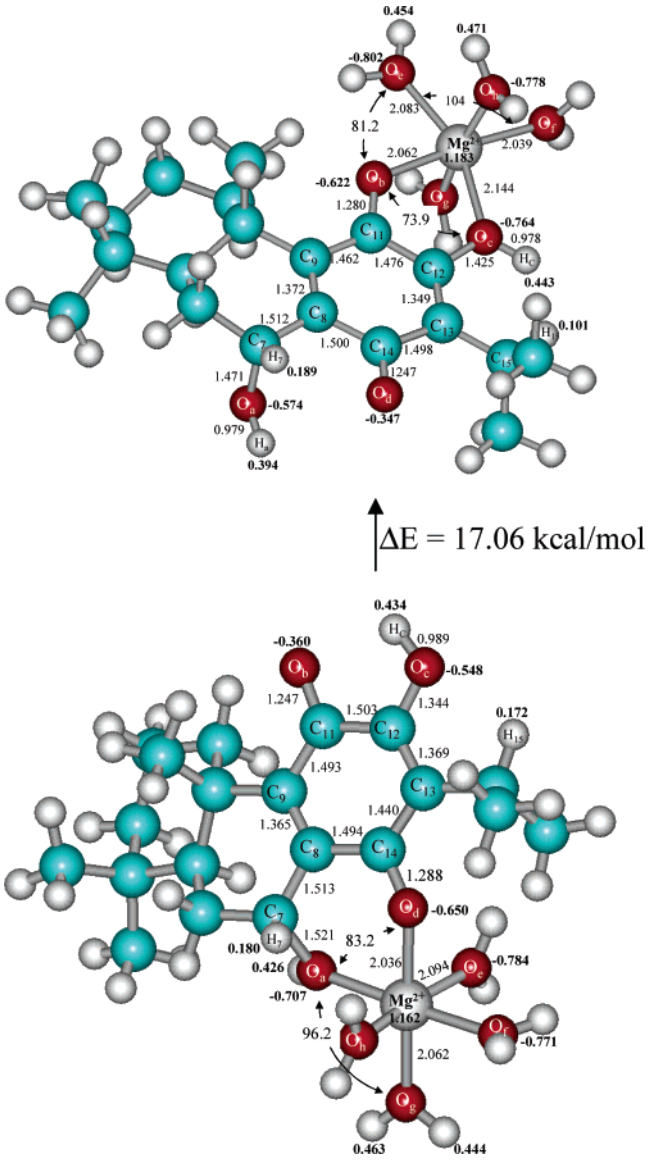

Figure 7. Optimized geometry for the [horminone(O_a−O_d)−Mg−(H_2O)$_4$]$^{2+}$ and [horminone(O_b−O_c)−Mg−(H_2O)$_4$]$^{2+}$ systems. Bond lengths, in Å, bond angles, in deg (in italics), and Mulliken populations, electron units (in bold characters), are indicated at the B3LYP/6-31G level.

[horminone(O_a−O_d)−Mg]$^{2+}$, ≅209 kcal/mol, is greater than that of [horminone(O_a−O_d)−Ca]$^{2+}$, ≅134 kcal/mol. Up to this point, the analyzed electronic and structural parameters account for the fact that horminone has more preference for Mg^{2+} than for Ca^{2+}.

Hydrated [Horminone−M−(H_2O)$_4$]$^{2+}$, M = Mg^{2+} and Ca^{2+}, Systems. The computed two low-lying states of the [horminone−Mg−(H_2O)$_4$]$^{2+}$ complex are shown in Figure 7. The lowest energy state arises when the ligand is coordinated through its O_a and O_d atoms to Mg^{2+}. Note that around the Mg^{2+} ion remains a slightly distorted octahedral geometry. The Mg−O_a and Mg−O_d bonding formation produces a reduction, from 90 to 83.2°, Table 3, for the O_a−Mg−O_d angle. Another O−Mg−O angle is 13° more opened; see Figure 7. On the other hand, as shown by the O−Mg−O bond angles (of 74−104°), in the higher energy [horminone(O_b−O_c)−Mg−(H_2O)$_4$]$^{2+}$ coordination mode occurs a highly distorted octahedral geometry around Mg^{2+}. This higher energy state was found 17 kcal/mol above the [horminone(O_a−O_d)−Mg−(H_2O)$_4$]$^{2+}$ state. This result should be compared with that one obtained in the absence of

TABLE 3: Selected O−M Bond Lengths, in Å, Bond O−M−O Angles, in deg, and Mulliken Populations for M^{2+} and Oxygen Atoms for the [Horminone(O_a−O_d)−M]$^{2+}$, [Horminone(O_b−O_c)−M]$^{2+}$, [Horminone(O_a−O_d)−M−(H_2O)$_4$]$^{2+}$, [Horminone(O_b−O_c)−M−(H_2O)$_4$]$^{2+}$, and [Horminone(O_a−O_d)−M−H_2O−$2H_3PO_4H_2PO_4$]$^+$ (M = Mg^{2+}, Ca^{2+}) Optimized Systems Using B3LYP/6-31G (M = Mg, Ca)

	bond				angle		charge				
complex	O_a−M	O_d−M	O_b−M	O_c−M	O_a−M−O_d	O_b−M−O_c	O_a	O_d	O_b	O_c	M
[horminone(O_a−O_d)−Mg]$^{2+}$	1.902	1.859			96.4		−0.803	−0.770			1.503
[horminone(O_b–O_c)−Mg)]$^{2+}$			1.899	1.971		82.9			−0.689	−0.780	1.503
[horminone(O_a−O_d)−Mg−(H_2O)$_4$]$^{2+}$	2.089	2.036			83.2		−0.707	−0.650			1.162
[horminone(O_b–O_c)−Mg−(H_2O)$_4$]$^{2+}$			2.062	2.144		73.9			−0.622	−0.764	1.183
[horminone(O_a−O_d)Mg−H_2O−$2H_3PO_4H_2PO_4$]$^+$	2.082	2.065			82.8		−0.731	−0.581			1.069
[horminone(O_a−O_d)−Ca]$^{2+}$	2.295	2.208			77.7		−0.798	−0.773			1.747
[horminone(O_b–O_c)−Ca]$^{2+}$			1.289	2.366		68.0			−0.738	−0.832	1.781
[horminone(O_a−O_d)−Ca−(H_2O)$_4$]$^{2+}$	2.411	2.360			73.2		−0.725	−0.663			1.480
[horminone(O_b–O_c)−Ca−(H_2O)$_4$]$^{2+}$			2.372	2.486		64.0			−0.641	−0.759	1.475
[horminone(O_a−O_d)Ca−H_2O−$2H_3PO_4H_2PO_4$]$^+$	2.404	2.360			72.0		−0.749	−0.619			1.413

TABLE 4: Calculated B3LYP/6-31G Binding Energies (BE) and Total ZPE Corrected Binding Energies (BE-ZPE), for the Horminone Complexes

complex	BE (kcal/mol)	BE-ZPE (kcal/mol)
[horminone(O_a−O_d)−Mg]$^{2+}$	209.87	209.02
[horminone(O_b−O_c)−Mg)]$^{2+}$	177.44	178.04
[horminone(O_a−O_d)−Mg−(H_2O)$_4$]$^{2+}$	401.05	387.82
[horminone(O_b−O_c)-Mg−(H_2O)$_4$]$^{2+}$	384.00	371.53
[horminone(O_a−O_d)Mg−H_2O−$2H_3PO_4H_2PO_4$]$^+$	599.12	
[horminone(O_a−O_d)−Ca]$^{2+}$	134.10	133.45
[horminone(O_b−O_c)−Ca]$^{2+}$	108.41	108.70
[horminone(O_a−O_d)−Ca−(H_2O)$_4$]$^{2+}$	302.27	290.65
[horminone(O_b−O_c)−Ca−(H_2O)$_4$]$^{2+}$	283.85	272.92
[horminone(O_a−O_d)Ca−H_2O−$2H_3PO_4H_2PO_4$]$^+$	500.50	

the first layer of water molecules. As quoted above, [horminone-(O_a−O_d)−Mg]$^{2+}$ and [horminone(O_b−O_c)−Mg]$^{2+}$ are separated by 32.4 kcal/mol, with the former one being also lower in energy.[18] A separation of 8.0 kcal/mol was obtained by the inclusion of the solvent effects through the PCM reaction field. In any case, the energy gap is high enough to be surmounted at room temperature. The importance of the direct inclusion of the water solvent effects is evident by the present results.

So, the more likely state of the hydrated horminone−Mg^{2+} complex is the one reported in Figure 7. The total binding energy of [horminone(O_a−O_d)−Mg−(H_2O)$_4$]$^{2+}$, of 401.05 kcal/mol, Table 4, is almost equal to that of [Mg(H_2O)$_6$]$^{2+}$, of 399.2 kcal/mol, suggesting an equilibrium of these two systems. However, the inclusion of zero point energy (ZPE) corrections produces binding energies of 387.82 and 380.31 kcal/mol for the former and later systems, respectively. That is, the horminone−Mg^{2+}−(H_2O)$_4$ complex is more stable, by 7.5 kcal/mol, than [Mg−(H_2O)$_6$]$^{2+}$. These B3LYP/6-31G results imply that horminone is able to displace two water molecules from the hexahydrated Mg^{2+} complex. This conclusion should be taken with caution, since, as quoted above for [Mg(H_2O)$_6$]$^{2+}$, huge changes (of nearly 80 kcal/mol) of binding energies are produced when going from the 6-31G basis set to the larger 6-311+G(2d,2p) one. Note that [horminone(O_b−O_c)−Mg−(H_2O)$_4$], 17 kcal/mol higher in energy, is unable to achieve such a displacement; see Figure 7. Then, a relatively stable complex [horminone(O_a−O_d)−Mg−(H_2O)$_4$]$^{2+}$ is formed when the horminone molecule is coordinated to Mg^{2+} through its O_a and O_d sites.

On the other hand, it has been determined that the oxytetracycline antibiotic crosses the wall cell of the bacteria in a cationic form, i.e., when it is bonded to a Mg^{2+} ion.[36] Since horminone is structurally related to oxytetracycline, the present results suggest that the horminone molecule may be able to penetrate the wall cell of the bacteria through the [horminone-(O_a−O_d)−Mg−(H_2O)$_4$]$^{2+}$ complex.

In the [horminone(O_a−O_d)−Mg−(H_2O)$_4$]$^{2+}$ ground state, the Mg−O distances fall in the 2.04−2.09 Å range. These values are shorter than the Mg−O distances of [Mg(H_2O)$_6$]$^{2+}$. In particular, Mg−O_d shows the shortest bond length, of 2.04 Å, and Mg−O_a has a 2.09 Å value; while Mg−O_g also shows a short value, of 2.06 Å. Then, the substitution of two H_2O units by horminone has promoted the appearance of shorter Mg−O bonds which can be accounted by the charge transfer, of 0.84 electrons, that is carried out from the water and horminone moieties toward Mg^{2+}. Note that, in the [horminone(O_b−O_c)−Mg−(H_2O)$_4$]$^{2+}$ higher energy state, a slightly smaller charge transfer, of 0.82 electrons, is observed, as well as the appearance of longer Mg−O bond lengths, of 2.04−2.14 Å.

The coordination of horminone with Mg^{2+} involves the formation of the six-member ring Mg^{2+}−O_a−C_7−C_8−C_{14}−O_d; see Figure 7. The Mg−O_d bond has a longer separation than Mg−O_a, which may be due to the fact that the oxygen O_a atom, bonded to a hydrogen atom, has a smaller capability for the transference of electrons toward Mg^{2+}. The O_a−C_7 (1.521 Å) and the O_d−C_{14} (1.288 Å) bond lengths are longer than their counterparts, 1.466 and 1.263 Å, of the bare horminone; see Figure 3. But the C_7−C_8 (1.513 Å) and the C_8−C_{14} (1.494 Å) bond lengths experience shortenings of 0.005 and 0.010 Å, respectively. So, this metal−ligand interaction has perturbed significantly the bonding of the O_a−C_7−C_8−C_{14}−O_d region. The C_8−C_9−C_{11}−C_{12}−C_{13}−C_{14} cycle, see Figure 7, has also been perturbed noticeably, since it shows enlargements of 0.003−0.013 Å and shortenings of 0.01−0.025 Å.

The structural changes quoted above are a consequence of the electronic effects that the [Mg(H_2O)$_4$]$^{2+}$ ion has produced on the horminone moiety, which are clearly exemplified by the oxygen atoms. In [horminone(O_a−O_d)−Mg−(H_2O)$_4$]$^{2+}$, the oxygen O_a and O_d, atoms, bonded to Mg^{2+}, have experienced a significant increase in their negative charge: from −0.61 (O_a) and −0.45 (O_d) electrons, in the bare horminone, they have increased up to −0.71 and −0.65 e1ectrons, respectively, in the hydrated complex. Then, at a first sight, in the Mg−O_a and Mg−O_d interactions, the metal to ligand back-donation is greater than the ligand to metal donation. On the other hand, the charge of the O atoms in [Mg−(H_2O)$_6$]$^{2+}$ is equal to −0.78, while in [horminone−Mg−(H_2O)$_4$]$^{2+}$, the O atoms (of the H_2O moieties) have values of −0.78 electrons, indicating the absence of changes in their atomic populations. That is, in the last complex the O atoms surrounding the Mg^{2+} ion are not responsible for the charge reduction of the metallic cation. Then, most of the donated charge to Mg^{2+} comes, ultimately, from the horminone molecule, producing, finally, the $Mg^{+1.16}$ cation. In fact, note that the O_b and O_c atoms, far away from the Mg^{2+} ion, experience a decrease in their electronic population. Even more,

TABLE 5: Selected O−H Bond Lengths, Å, and Mulliken Populations for Hydrogen Atoms for the Horminone, [Horminone(O_a−O_d)−Mg]$^{2+}$, [Horminone(O_a−O_d)−Mg−(H_2O)$_4$]$^{2+}$, and [Horminone(O_a−O_d)−Mg−H_2O−$2H_3PO_4H_2PO_4$]$^+$ Optimized Systems Using B3LYP/6-31G

	charge			
atom	horminone	horminone (O_a−O_d)−Mg^{2+}	horminone (O_a−O_d)−Mg^{2+}−$4H_2O$	horminone (O_a−O_d)−Mg^{2+}−H_2O−$2H_3PO_4H_2PO_4$
$H_7(C_7)$	0.149	0.224	0.180	0.211
$H_a(O_a)$	0.380	0.467	0.426	0.486
$H_{15}(C_{15})$	0.167	0.208	0.172	0.185
$H_{20a}(C_{20})$	0.158	0.208	0.179	0.170
$H_{20b}(C_{20})$	0.132	0.147	0.141	0.137
$H_{20c}(C_{20})$	0.145	0.194	0.182	0.162
$H_c(O_c)$	0.401	0.447	0.434	0.417
	bond length			
bond	horminone	horminone (O_a−O_d)−Mg^{2+}	horminone (O_a−O_d)−Mg^{2+}−$4H_2O$	horminone (O_a−O_d)−Mg^{2+}−H_2O−$2H_3PO_4H_2PO_4$
O_a−H_a	0.982	0.977	0.977	0.992
O_c−H_c	0.989	0.991	0.989	0.989

most of the H atoms of the horminone molecule, with respect to the bare state of this moiety, have experienced a significant decrease in their electronic charge. See for instance, in Figures 3 and 7, the indicated populations of the H atoms, particularly those of H_c, H_{15}, and H_7. This picture suggests that the whole electronic cloud of the horminone moiety has been strongly polarized toward the O_a−Mg−O_d region; see Table 5. The direct effects of the solvent water molecules are clearly seen by these results.

For [horminone−Ca−(H_2O)$_4$]$^{2+}$ also the O_a−Ca−O_d and O_b−Ca−O_c coordinations were searched. The B3LYP/6-31G results indicates that [horminone(O_a−O_d)−Ca−(H_2O)$_4$]$^{2+}$ is 18.4 kcal/mol more stable than [horminone(O_b−O_c)−Ca−(H_2O)$_4$]$^{2+}$; see Figure 8. This energy gap is quite similar to that found for the Mg^{2+} case; see Figure 7. However, in the ground and higher energy states of the Ca^{2+} complex, occur highly distorted octahedral geometries around the Ca^{2+} ion, which reflects a weaker bonding metal−ligand behavior.

The [horminone(O_a−O_d)−Ca−(H_2O)$_4$]$^{2+}$, 302.27 (290.65) kcal/mol, binding energy is almost equal to that of [Ca(H_2O)$_6$]$^{2+}$, 301.5 (288.1) kcal/mol, values in parentheses including ZPE corrections, implying that horminone is in equilibrium with the hexahydrated Ca^{2+} complex. However, the [horminone-(O_a−O_d)−Ca−(H_2O)$_4$]$^{2+}$ binding energy is substantially smaller, by about 100 kcal/mol, than the corresponding value, 401.05 (387.82) kcal/mol, of [horminone(O_a−O_d)−Mg−(H_2O)$_4$]$^{2+}$. These results are in agreement with the calculated Ca−O bond lengths, 2.36−2.41 Å, which are substantially longer than the Mg−O values, of 2.04−2.09 Å. Moreover, a significant smaller charge transfer, of 0.55 electrons, has occurred in the calcium complex than in the magnesium one, of 0.84 electrons. That is, the Mg^{2+} ion (66 pm) small size leads to a strong electrostatic attraction for the oxygen atoms of the ligands (horminone and water moieties), while the larger size of the Ca^{2+} ion (99 pm) leads to much smaller interaction energies.[37] So, these energetic, structural, and electronic parameters account for the fact that the horminone molecule has more preference for Mg^{2+} ion than for Ca^{2+}. On the other hand, the reported hardness values of the Mg^{2+} and Ca^{2+} ions[38] are 32.55 and 19.52 eV, respectively, while horminone has a 1.55 eV value; this last value was estimated as half the difference between the LUMO and HOMO orbital energies. So, these two metal ions and horminone present

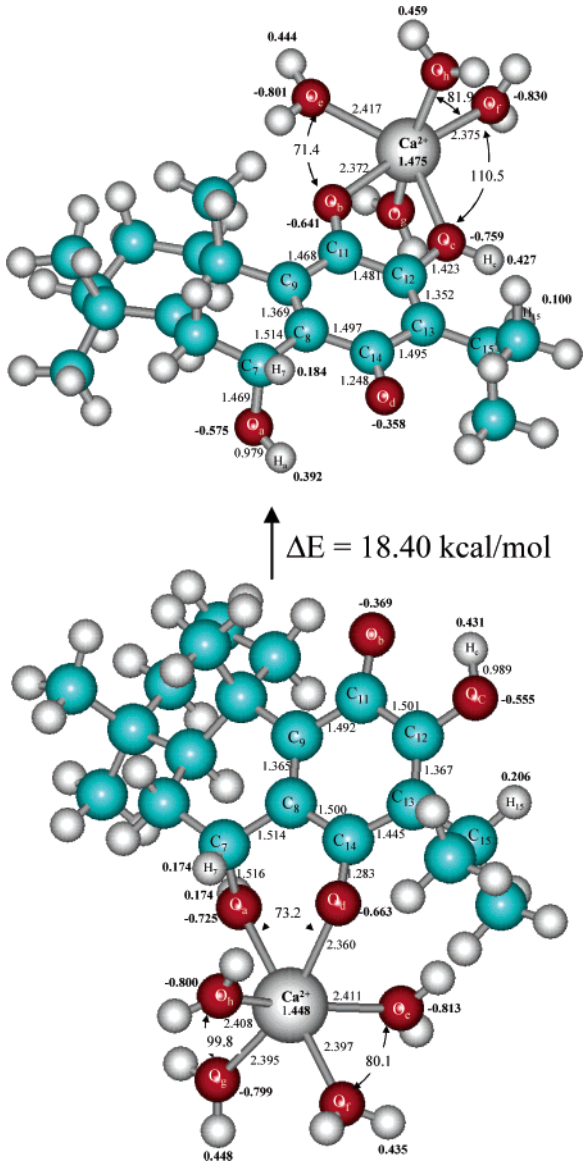

Figure 8. Optimized geometry for the [horminone(O_a−O_d)−Ca−(H_2O)$_4$]$^{2+}$ and [horminone(O_b−O_c)−Ca−(H_2O)$_4$]$^{2+}$ systems. Bond lengths, in Å, bond angles, in deg (in italics), and Mulliken populations, electron units (in bold characters), are indicated at the B3LYP/6-31G level.

a great difference in hardness, indicating low metal−ligand reactivity. As for horminone, we have also estimated the [Mg(H_2O)$_6$]$^{2+}$ and [Ca(H_2O)$_6$]$^{2+}$ hardness. The results are 4.68 and 4.34 eV, respectively, indicating that, in the hexahydrated fashion, these ions are more likely to react with the horminone moiety. We will continue with the discussion of the [horminone(O_a−O_d)−Mg−(H_2O)$_4$]$^{2+}$ and [horminone(O_a−O_d)−Ca−(H_2O)$_4$]$^{2+}$ lowest energy states.

[Horminone−M−(H_2O)(PO_4H_2)(PO_4H_3)$_2$]$^+$, M = Mg^{2+} and Ca^{2+}. Up to here, we have studied the bonding of the horminone molecule to the Mg^{2+} and Ca^{2+} ions, taking into account explicitly the effects of the first layer of H_2O molecules. The obtained results indicate that horminone has greater preference for Mg^{2+} than for Ca^{2+}. As quoted above, through the attachment of horminone to the hydrated Mg^{2+} ion, this antibiotic crosses the membrane wall; once inside the inhibition of the protein synthesis initiates. As it was mentioned in the Introduction, the horminone molecule is structurally related to the family of the tetracycline molecules. It has been found that the divalent magnesium is crucial for the binding of the

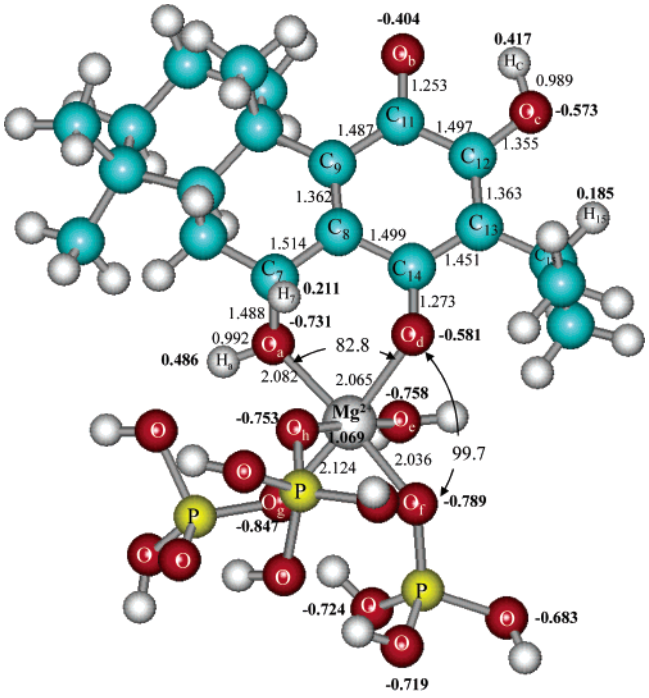

Figure 9. Optimized geometry for the [horminone(O_a−O_d)−Mg^{2+}−H_2O−$2H_3PO_4H_2PO_4$]$^+$ system. Bond lengths, in Å, bond angles in deg (in italics), and Mulliken populations, electron units (in bold characters), are indicated at the B3LYP/6-31G level.

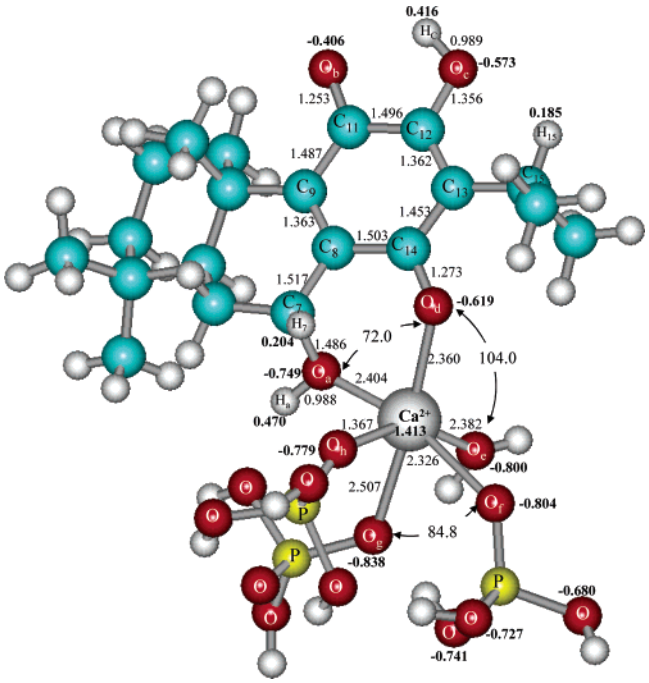

Figure 10. Optimized geometry for the [horminone(O_a−O_d)−Ca^{2+}−H_2O−$2H_3PO_4H_2PO_4$]$^+$ system. Bond lengths, in Å, bond angles in deg (in italics), and Mulliken populations, electron units (in bold characters), are indicated at the B3LYP/6-31G level.

tetracycline antibiotics to the ribosome. Specifically, the tetracycline drug interacts with the phosphate oxygen atoms of the RNA residues.[20] Therefore, we have also studied the interaction of the hydrated horminone−Mg^{2+} system with the phosphate, PO_4^{3-}, groups of ribosomes, which implies the displacement of three H_2O molecules from [horminone(O_a−O_d)−Mg−$(H_2O)_4$]$^{2+}$, yielding the [horminone(O_a−O_d)−Mg−(H_2O)-$(PO_4H_2)(PO_4H_3)_2$]$^+$ complex, where the oxygen atoms of the PO_4^{3-} groups have been saturated with protons. The optimized geometry of this system is shown in Figure 9. Also here, as in [horminone(O_a−O_d)−Mg−$(H_2O)_4$]$^{2+}$, remains some type of octahedral symmetry around Mg^{2+}. Despite the fact that the Mg−O bonds are originated from the interaction of the Mg^{2+} ion with three different ligands (horminone, phosphate, and H_2O), the Mg−O bond lengths are restrained within the 2.065−2.124 Å range. On average, the Mg−O_a and Mg−O_d bonds are slightly shorter than the Mg−O(phosphate) bonds. With the remaining H_2O molecule, the Mg^{2+} ion has a 2.071 Å Mg−O bond; this value is even shorter than the corresponding values in [horminone(O_a−O_d)−Mg−$(H_2O)_4$]$^{2+}$ and in [Mg−$(H_2O)_6$]$^{2+}$. Overall, this Mg−O bond contraction indicates a greater bonding interaction between the Mg^{2+} cation and the horminone molecule in the [horminone(O_a−O_d)−Mg−$(H_2O)(PO_4H_2)$-$(PO_4H_3)_2$]$^+$ complex, where a charge transfer occurs, of 0.93 electrons, from the ligands toward Mg^{2+}. The calculated binding energy is 599.10 kcal/mol. The values of these two properties are bigger than those observed in [horminone(O_a−O_d)−Mg−$(H_2O)_4$]$^{2+}$ and in [$Mg(H_2O)_6$]$^{2+}$, which accounts for the stability of the horminone−Mg^{2+}−phosphate complex. With longer Ca−O distances, of 2.33−2.51 Å, and a smaller charge transfer, of 0.59 electrons, the binding energy (500.5 kcal/mol) of the Ca^{2+} complex, [horminone(O_a−O_d)−Ca−$(H_2O)(PO_4H_2)$-$(PO_4H_3)_2$]$^+$, shown in Figure 10, is significantly smaller than that of the corresponding Mg^{2+} system. This implies that, through the Mg^{2+} ion, the horminone antibiotic can be bonded to RNA. Further, such horminone−Mg^{2+} to RNA attachment may produce the inhibition of the protein synthesis.

Conclusions

The coordination of the horminone molecule with hydrated magnesium and calcium divalent ions was studied by means of the B3LYP/6-31G method. The first layer of water molecules surrounding the metallic cations was included. The hydrated Mg^{2+} and Ca^{2+} ions exhibit a quite different structural and energetic coordination behavior with horminone. It was found that the octahedral [horminone(O_a−O_d)−Mg−$(H_2O)_4$]$^{2+}$ unit is more stable, by 7.5 kcal/mol, than [$Mg(H_2O)_6$]$^{2+}$. That is, the moderate B3LYP/6-31G level of theory indicates that horminone is able to displace two water molecules from the hexahydrated complex. This behavior does not occur for Ca^{2+}. Consistently, [horminone(O_a−O_d)−Mg−$(H_2O)_4$]$^{2+}$ has a greater, by about 100 kcal/mol, metal−ligand binding energy than [horminone-(O_a−O_d)−Ca−$(H_2O)_4$]$^{2+}$. The preference of horminone by Mg^{2+} is enlightened by these results. Moreover, its electronic structure, as shown by huge changes in the atomic populations, is strongly perturbed by Mg^{2+}. The small size of the Mg^{2+} ion (66 pm) leads to a strong electrostatic attraction of the oxygen atoms of the ligands (horminone and water moieties), while the larger size of the Ca^{2+} ion (99 pm) leads to much smaller interaction energies. Indeed, horminone, bounded to [Mg-$(H_2O)_4$]$^{2+}$ is able to cross the bacterial membrane cell. Once inside, [horminone(O_a−O_d)−Mg−$(H_2O)_4$]$^{2+}$ binds to the rRNA phosphate groups yielding [horminone(O_a−O_d)−Mg−(H_2O)-$(PO_4H_2)(PO_4H_3)_2$]$^+$. The attachment of horminone to mRNA may inhibit the mechanism involved in the protein synthesis. Overall, these results account for the fact that since ancient times *Salvia* species, to which horminone belongs, have been used in folk medicine all around the word due to their diverse biological activities, including antibacterial and antituberculous. The present results suggest that such antibacterial activity is mainly due to the attachment of horminone to the Mg^{2+} ion and,

furthermore, to the binding of the hydrated horminone−Mg^{2+} complex to the mRNA phosphate groups.

Acknowledgment. I.N. acknowledges a grant from the CONACYT and DGPA-UNAM (PASPA). M.C. acknowledges financial support from the DGAPA-UNAM under the PAPIIT-IN-107905 Project. The access to the supercomputer SG Origin 2000/32 at DGSCA-UNAM is strongly appreciated.

Supporting Information Available: Details of theoretical calculations including total energies (au) of selected fully optimized compounds, with Cartesian coordinates indicated at the B3LYP/6-31G level. This material is available free of charge via the Internet at http://pubs.acs.org.

References and Notes

(1) Hansch, C. *Acc. Chem. Res*. **1969**, *2*, 232.
(2) Hansch, C.; Klein, T. E. *Acc. Chem. Res*. **1986**, *19*, 392.
(3) Greco, G.; Novellino, E.; Silipo, C.; Vittoria, A. *Quant. Struct.-Act. Relat*. **1992**, *11*, 461.
(4) Martínez-Vázquez, M.; Miranda, P.; Valencia, N. A.; Torres, M. L.; Miranda, R.; Cárdenas, J.; Salmón, M. *Pharm. Biol*. **1998**, *36*, 77.
(5) Janot, M. M.; Potier, P. *Ann. Pharm. Fr*. **1964**, *22*, 387.
(6) Edwards, O. E.; Feniak, G.; Los, M. *Can. J. Chem*. **1962**, *40*, 1540.
(7) Batista, O.; Duarte, A.; Nascimento, J.; Simões, M. F.; De La Torre, M. C.; Rodríguez, B. *J. Nat. Prod. 1994*, *57*, 858.
(8) Ulubelen, A.; Öksüz, S.; Kolak, U.; Tan N.; Bozok-Johansson, C.; Çelik, C.; Kohlbau, H.-J.; Voelter, W. *Phytochemistry* **1999**, *52*, 1455.
(9) Ulubelen, A.; Öksüz, S.; Topcu, G.; Gören, A. C.; Voelter, W. *J. Nat. Prod*. **2001**, *64*, 549.
(10) Jonathan, L. T.; Che, C.-T.; Pezzuto, J. M.; Fong, H. H. S.; Farnsworth, N. R. *J. Nat. Prod*. **1989**, *52*, 571.
(11) Goijman, S. G.; Turrens, J. F.; Marini-Bettolo, G. B.; Stoppani, A. O. M. *Experentia* **1985**, *41*, 646.
(12) Putnam, L. E.; Hendricks, F. D.; Welch, H. *Antibiot. Chemother*. **1953**, *3*, 1183.
(13) Nelson, M. L.; Park, B. H.; Levy, S. B. *J. Med. Chem*. **1994**, *37*, 1355.
(14) Othersen O. G.; Lanig H.; Clark T. *J. Med. Chem*. **2003**, *46*, 5571.
(15) Ohyama, T.; Cowan, J. A. *Inorg. Chem*. **1995**, *34*, 3083.
(16) Degenkolb, J.; Takahashi, M.; Ellestad, G. A.; Hillen, W. *Antimicrob. Agents Chemother*. **1991**, *35*, 1591.
(17) Gesteland, R. F.; Atkins, J. F. *The RNA World*; Cold Spring Harbor Laboratories: Cold Spring Harbor, NY, 1993; Chapter 12, pp 271−302.
(18) Nicolás, I.; Vilchis, M. B.; Aragón, N.; Miranda, R.; Hojer, G.; Castro, M. *Int. J. Quantum Chem.* **2003**, *93*, 411.
(19) Bock, C. W.; Katz, A. K.; Glusker, J. P. *J. Am. Chem. Soc*. **1995**, *117*, 3754.
(20) Brodersen, D. E.; Clemons, W. M., Jr.; Carter, A. P.; Morgan-Warren, R. J.; Wimberly, B. T.; Ramakrishnan, V. *Cell* **2000**, *103*, 1143.
(21) (a) Bock, C. W.; Glusker, J. P. *Inorg. Chem*. **1993**, *32*, 1242. (b) Bock, C. W.; Kaufman, A.; Glusker, J. P. *Inorg. Chem*. **1994**, *33*, 419.
(22) Markham, G. D.; Glusker, J. P.; Bock, C. L.; Trachtman, M.; Bock, C. W. *J. Phys. Chem*. **1996**, *100*, 3488.
(23) Katz, A. K.; Glusker, J. P.; Beebe, S. A.; Bock, C. W. *J. Am. Chem. Soc*. **1996**, *118*, 5752.
(24) Carugo, O.; Djinoviæ, K.; Rizzi, M. *J. Chem. Soc., Dalton Trans*. **1993**, 2127.
(25) Pavlov, M.; Siegbahn, P. E. M.; Sandström, M. *J. Phys. Chem. A* **1998**, *102*, 219.
(26) Lee, C.; Yang, W.; Parr, R. G. *Phys. Rev.* B **1988**, *37*, 785.
(27) Becke, A. D. *J. Chem. Phys*. **1993**, *98*, 5648.
(28) Hehre, W. J.; Ditchfield, R.; Pople, J. A. *J. Chem. Phys*. **1972**, *56*, 2257.
(29) a) Frisch, M. J.; Pople, J. A.; Binkley, J. S. *J. Chem. Phys.* **1984**, *80*, 3265. (b) Krishnan, R.; Binkley, J. S.; Seeger, R.; Pople, J. A. *J. Chem. Phys*. **1980**, *72*, 650.
(30) Francl, M. M.; Pietro, W. J.; Hehre, W. J.; Binkley, J. S.; Gordon, M. S.; DeFrees, D. J.; Pople, J. A. *J. Chem. Phys*. **1982**, *77*, 3654.
(31) Frisch, M. J.; Trucks, G. W.; Schlegel, H. B.; Scuseria, G. E.; Robb, M. A.; Cheeseman, J. R.; Zakrzewski, V. G.; Montgomery, J. A., Jr.; Stratmann, R. E.; Burant, J. C.; Dapprich, S.; Millan, J. M.; Daniels, A. D.; Kudin, K. N.; Strain, M. C.; Farkas, O.; Tomasi, J.; Barone, V.; Cossi, M.; Cammi, R.; Mennucci, B.; Pomelli, C.; Adamo, C.; Clifford, S.; Ochterski, J.; Peterson, G. A.; Ayala, P. Y.; Cui, Q.; Morokuma, K.; Malick, D. K.; Rabuck, A. D.; Raaghavachari, K.; Foresman, J. B.; Cioslowski, J.; Ortiz, J. V.; Baboul, A. G.; Stefanov, B. B.; Liu, G.; Liashenko, A.; Piskorz, P.; Komaromi, I.; Gomperts, R.; Martin, R. L.; Fox, D. J.; Keith, T.; Al-Laham, M. A.; Peng, C. Y.; Nanayahkara, A.; González, C.; Challacombe, M.; Gill, P. M. W.; Jhonson, B.; Chen, W.; Wong, M. W.; Andres, J. L.; Head-Gordon, M.; Replogle, E. S.; Pople, J. A. *Gaussian 98*, revision A.7; Gaussian: Pittsburgh, PA, 1998.
(32) Boys, S. F.; Bernardi, F. *Mol. Phys*. **1970**, *19*, 553.
(33) Bader R. F. W. *Atoms in Molecules. A Quantum Theory*; Clarendon: Oxford, U.K., 1990.
(34) AIM2000 was designed by Friedrich Biegler-König, University of Applied Sciences, Bielefeld, Germany, 2000.
(35) Miertus, S.; Scrocco, E.; Tomasi, J. *Chem. Phys*. **1981**, *55*, 117.
(36) Schnappinger, D.; Hillen, W. *Arch. Microbiol*. **1996**, *165*, 359.
(37) Schmitt, M. O.; Schneider, S. *Phys. Chem. Commun*. **2000**, *9*, 1.
(38) Pearson, R. G. *Inorg. Chem*. **1988**, *27*, 734.